Effect of Tibial Tuberosity Advancement on the Contact Mechanics and the Alignment of the Patellofemoral and Femorotibial Joints

Tomás G. Guerrero*,[1], Dr. Med Vet, Diplomate ECVS, Antonio Pozzi*,[2], DMV, MS, Diplomate ACVS, Nicholas Dunbar[3], BS, Nicolas Kipfer[1], Dr. Med Vet, Michael Haessig[4], Dr. Med Vet, Diplomate ECVPH & ECBHM, Mary Beth Horodyski[5], ATC, and Pierre M. Montavon[1], Dr. Med Vet

[1]Clinic for Small Animal Surgery, Vetsuisse-Faculty University of Zurich, Zurich, Switzerland, [2]Department of Small Animal Clinical Sciences and the Collaborative Orthopaedic Biomechanical Laboratory, University of Florida, Gainesville, FL, [3]Department of Mechanical and Aerospace Engineering and the Collaborative Orthopaedic Biomechanical Laboratory, University of Florida, Gainesville, FL, [4]Department of Herd Health Management. Vetsuisse-Faculty University of Zurich, Zurich, Switzerland and [5]Department of Orthopedics and Rehabilitation and the Collaborative Orthopaedic Biomechanical Laboratory, University of Florida, Gainesville, FL

Corresponding Author
Dr. Tomás G. Guerrero, Dr. Med Vet, Diplomate ECVS, Small Animal Medicine & Surgery Academic Program, St. George's University, School of Veterinary Medicine, True Blue, Grenada, West Indies
E-mail: tguerrero@sgu.edu

Submitted December 2009
Accepted April 2010

DOI:10.1111/j.1532-950X.2011.00866.x

Objective: To evaluate the effect of tibial tuberosity advancement (TTA) on patellofemoral (PF) contact mechanics, and alignment of the PF and femorotibial (FT) joints in cranial cruciate ligament (CrCL)-deficient stifles of dogs.
Study design: Ex vivo biomechanical study.
Animals: Unpaired cadaveric hind limbs (n = 9).
Methods: Digital pressure sensors placed in the PF joint were used to measure contact force, contact area, peak and mean contact pressure, and peak pressure location with the limb under an axial load of 30% body weight and a stifle angle of 135°. The FT and PF poses were obtained using a 2-dimensional computer digitization technique. Each specimen was tested under normal, CrCL-deficient, and TTA-treated conditions. Data was normalized and analyzed, after testing for normality by Wilk–Shapiro, using 1 sample T-test, paired T-test, and ANOVA; $P \leq .05$ was considered significant. Bonferroni's correction was used when needed.
Results: A significant cranioproximal tibial displacement and increase in patellar tilt were found in the CrCL-deficient joints. Both FT and PF alignments were restored after TTA. Contact areas and peak pressure did not vary between conditions. Peak pressure location displaced proximally from intact to CrCL-deficient condition and returned to normal after TTA. Total force measured in the CrCL-deficient stifle and TTA conditions were significantly lower than in the control.
Conclusion: TTA restored the normal FT and PF alignment, and reduced the retropatellar force by about 20%.

The high incidence of cranial cruciate ligament (CrCL) insufficiency in dogs has led to the development of numerous surgical techniques in attempt to improve clinical results.[1–5] Traditional surgical techniques attempt to stabilize the joint by replacing the CrCL with a structure that mimics its function. Tibial osteotomies differ from the traditional stabilization techniques because they aim to create dynamic stability by altering bone geometry. Tibial tuberosity advancement (TTA), developed at the University of Zurich in 2002,[6–8] attempts to restore dynamic stability in CrCL-deficient stifles by reducing the angle formed by the patellar tendon and the tibial plateau (PTA). Stability is accomplished by performing an osteotomy of the tibial tuberosity in the frontal plane and advancing the bone fragment. The magnitude of advancement is based on the preoperative PTA and depends on the size of spacers placed in the gap of the osteotomy.[8]

The biomechanics of the TTA has been studied in ex vivo experiments evaluating the kinematics and contact mechanics of the femorotibial (FT) joint.[9–12] These studies

Presented at the 37th Annual Conference Veterinary Orthopedic Society, Breckenrigde, CO, 2010, February 20–27, 2010 and at the 19th ECVS Annual Scientific Meeting. Helsinki, Finland, July 1–3, 2010.
This work was performed at the Vetsuisse-Faculty University of Zurich, and at the University of Florida Comparative Orthopaedics and Biomechanics Laboratory.
*Contributed equally.

have demonstrated that the FT shear force shifts from cranial to caudal direction at a critical point of about 90° of PTA.[10–13] A more recent study evaluating the 3-dimensional kinematics and the contact mechanics of the CrCL-deficient stifle stabilized by TTA found that both normal alignment and contact pressures were achieved with TTA in a static ex vivo model.[9] Whereas the effect of TTA on FT biomechanics has been extensively studied, patellofemoral (PF) biomechanics after TTA is unknown.

Osteoarthritis of the PF joint occurs in dogs with naturally occurring and experimentally-induced CrCL insufficiency,[14,15] with cartilage hypertrophy being observed in this joint shortly after experimental CrCL transection.[15] A recent study reported that 34 of 40 stifles of dogs with CrCL insufficiency suffered from different degrees of cartilage damage in the PF joint.[14] Osteoarthritis of the PF joint causing "femoropatellar pain syndrome" is also common in people.[16–20] In an attempt to alleviate retropatellar pain, in 1976 Maquet[21] described the anterior displacement of the tibial tubercle technique to treat PF arthralgias. By advancing the tibial tubercle, the moment arm of the patellar tendon is increased and therefore the forces needed to extend the knee, and acting in the PF joint are reduced.[22,23] The biomechanics of the technique have been validated in ex vivo cadaveric studies,[22,24–27] and clinical studies have shown reduction of pain in the joint.[28–31]

Advancement of the tibial tuberosity in combination with lateralization or medialization, was originally described in dogs to decrease retropatellar pressure during the surgical treatment of patellar luxation.[32–34] One of the advantages of TTA is that it may decrease the retropatellar pressure while providing dynamic stability to the FT joint. Decreased retropatellar pressure may relieve pain and decrease the progression of PF cartilage degeneration.[5,14,35,36] We are unaware of studies evaluating the contact mechanics and alignment of the PF joint in the normal stifle, after CrCL transection (CrCLT) and after TTA stabilization. Our purpose was to evaluate the effects of TTA on PF contact mechanics and alignment in a static model mimicking the weight-bearing phase of the gait. We hypothesized that TTA, while restoring normal FT and PF alignment, would reduce retropatellar force when compared with CrCL-intact stifles. We also hypothesized that CrCLT would cause a decrease in retropatellar pressure and a shift in peak pressure. In order to test our hypothesis, we evaluated FT and PF alignment using a 2-dimensional digitization technique applied to radiographs; we also measured retropatellar contact pressures, forces, and areas using a pressure sensor placed in the PF joint.

MATERIALS AND METHODS

Specimen Preparation

Nine stifles of 6 adult dogs that died or were euthanatized for causes unrelated to this study were harvested by disarticulation at the coxofemoral and tibiotarsal joint. Standard orthogonal radiographic projections were taken of each limb to ensure that the stifles were free of orthopedic disease and for measurement of the PTA and preoperative planning of the TTA.[8,37,38] The required advancement was measured using the common tangent method.[13,39] The soft tissue surrounding the limbs was removed carefully, preserving the stifle joint capsule, the patella, the patellar ligament, and the collateral ligaments. Each limb was wrapped in saline-moistened towels, sealed in plastic bags, and stored at −80°C. Twenty-four hours before testing, each specimen was thawed in a refrigerator. On the day of testing, stainless steel beads of 1 mm diameter (Hasler+CO AG Oerlikon, Zurich, Switzerland) acting as radiodense markers, were impacted at the femoral and tibial attachments of the medial collateral ligament[12] in the medial aspect of the patella and in the medial trochlear ridge of the femur. TTA was performed in each leg using commercially available implants and instruments (Kyon AG, Zurich, Switzerland) before mounting the leg in the testing apparatus (Fig 1). The distal screw holes of the plate were drilled

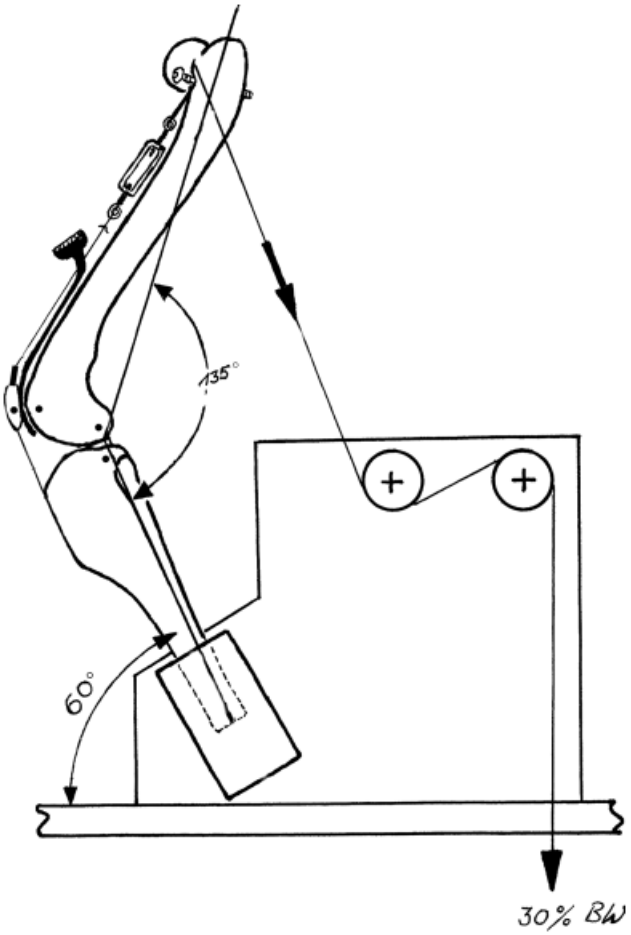

Figure 1 Illustration of the testing apparatus including, bone markers, Pliance® sensor positioned in the femoropatellar joint, and a turnbuckle link extending from a screw positioned in the proximal femur to the tendon of insertion of the quadriceps in the patella. The distal tibia was potted in polymethylmethacrylate and clamped at 60° to a horizontal plane into the socket of a jig fixed to a table.

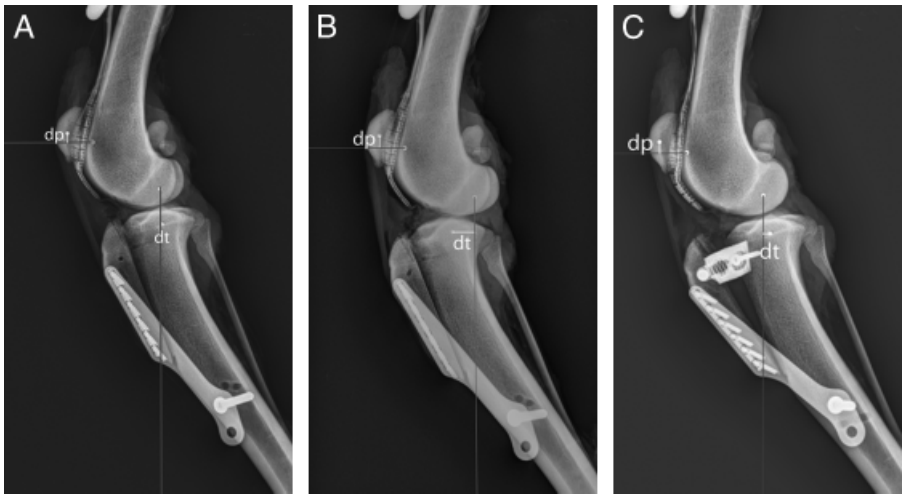

Figure 2 Mediolateral radiographic images of one specimen in the intact condition (A), after CrCl transection (B), and after TTA (C). The markers in the proximal tibia, and at the insertion of the medial collateral ligament in the femur were used to assess cranial tibial subluxation. The horizontal distance between the tibial marker and the vertical passing through the femoral marker ''dt,'' was measured and compared between conditions. Cranial tibial subluxation is observed in (B), and slightly overcorrection is seen in (C). The markers in the femoral trochlea and in the patella were used in the same way to detect proximo-distal displacement of the patella related to the femur. The segment ''dp'' was defined as the vertical distance between the patellar marker and the horizontal line passing by the marker positioned in the femoral trochlea. Two holes were drilled in the body of the tibia to fix the distal end of the plate. In the sham and CrCLT conditions the distal hole was used, and after TTA the plate was fixed to the proximal hole to avoid changing the position of the patella.

in the body of the tibia at 2 different levels to fix the plate in a sham-position without tuberosity advancement, and in a position that would stabilize the osteotomy at the planned amount of distraction that resulted in a PTA of 90° (TTA condition). During drilling this last hole the patella was fixed to the femur with bone reduction forceps, the tibial tuberosity was rotated around it, and at the same time was allowed to displace proximally. In this way, proximal or distal displacement of the patella after TTA was avoided (Fig 2).

A digital pressure sensor (Pliance® S2070 sensor, Pliance®-x system, Pliance, Munich, Germany) was placed in the PF joint and fixed by gluing and suturing the peripheral tabs to the joint capsule. This system consisted of a custom-designed, plastic laminated film, an electronic pressure sensor, a sensor handle, and software for data acquisition and analysis. The sensor had 34 sensing elements distributed in a sensing area of 458 mm^2. The sensors had a pressure sensitivity of 0.01 MPa, and a pressure range of 0.05–2 MPa.

Testing Protocol

The specimens were positioned in a custom-designed aluminum testing apparatus and loaded to replicate the stance phase of a walking gait, as described previously.[11] The distal extremity of the tibia was potted in polymethylmethacrylate and clamped at 60° to the horizontal plane into the socket of a jig fixed to a table.[11] A turnbuckle link extending from a screw positioned in the proximal femur and sutured with UPS 6 polyglactin 910 using a tension suture pattern to the tendon of insertion of the quadriceps in the patella simulated the quadriceps mechanism. This turnbuckle was corrected between each condition to keep always the stifle at an angle of approximately 135° of extension corresponding to the mid-point of stance phase of the walking.[40] This angle was measured with a goniometer using as landmarks the greater trochanter of the femur, the FT joint between the lateral epicondyle of the femur and the fibular head and the lateral malleolus of the distal tibia.[40,41] A kevlar line (AHF Leitner, Pfaffenhofen, Germany) was attached from the proximal femur to a metal tray where weights representing 30% of the body weight of the dog were placed.[11]

Loading and data acquisition were performed in the following sequence: (1) normal (CrCL-intact, sham TTA), (2) CrCLT (CrCLT, sham TTA), and (3) TTA-treated (CrCLT, TTA-treated). For testing conditions (2) and (3), the CrCL was transected at its origin by a craniomedial approach to the stifle. At each of the 3 conditions contact mechanics measurements were recorded and mediolateral radiographs were taken.

Contact Mechanics

Contact area, peak contact pressure and location, mean pressure and total force measurements in the PF joint were acquired with the digital pressure sensing system. Contact area was defined as the area of contact between the femoral sulcus and the patella. Peak contact pressure was defined as the highest pressure measured in the contact area. Pressure distribution was described according to the location of the center of the peak contact pressure: the relative location of the peak pressure for each condition was defined as the

distance from the peak pressure sensel to the original position in the intact stifle. Mean pressure represented the average of the pressures across the contact area. Total force was defined as the magnitude of load transmitted across the PF joint.

Contact area, peak contact pressure and location, mean pressure and total force were acquired for each testing condition after 5 seconds of holding peak force. Contact area values were expressed in cm^2, peak and mean contact pressure were expressed in kPa, and total force was expressed in N. The obtained measurements of contact mechanics were normalized to the measurements taken in the intact condition, which were defined as 100%. After normalization the values were expressed as a percentage of the control. Peak pressure location was measured and expressed in mm.

FT and PF Joints Alignment

The position of the tibia relative to the femur was evaluated on mediolateral radiographs using a previously described method.[12] The position of the sensor was also confirmed on the radiographs before and during testing. After being exported as uncompressed tagged-image file format files, the images were analyzed using a commercial software (Adobe Photoshop 7.0, Adobe Systems Inc., Seattle, WA). Measurement of tibial translation was accomplished by measuring the initial horizontal distance of the tibial marker from the femoral markers to establish the control position (Fig 2A). After each treatment, marker distance was remeasured, and horizontal displacement relative to the control position was calculated (Fig 2B and C).[12]

The alignments of the PF and FT joints were also evaluated with a custom computer digitization technique. Radiographic analysis was performed using previously documented digitization techniques designed to reliably construct a femoral coordinate system to measure the positions of the patella and tibia (Fig 3A and B).[42] Calculations were performed on a custom written computer program using Matlab (The MathWorks Inc., Natick, MA). Images were calibrated using the known length of the TTA plate in each radiograph. The measured length of the plate was selected because considered capable of accommodating small out of plane rotations.

A distal femur axis was constructed using the femoral condyle length (FCL). The FCL was defined as the perpendicular distance between a line parallel to the proximal cranial cortex of the femur and the midpoint of the 2 most caudal points on the femoral condyles.[43] Two arcs were constructed with an origin at the proximal aspect of the trochlea and radii equal to 1 and 1.5 times the FCL, respectively. The long axis of the distal femur was defined as the line connecting the midpoints between the intersections of each arc and each cortex (Fig 3C).

A proximal tibial axis was constructed to approximate the standard tibial reference axis without the use of the talus.[43,44] The proximal tibial width (PTW) was defined as the length between the proximal-most aspect of the tibial tuberosity and caudal-most aspect of the tibial condyles. An arc was constructed with an origin at the cranial-most aspect of the articular surface of the proximal tibia with a radius of 2 times PTW. The long axis of the proximal tibia

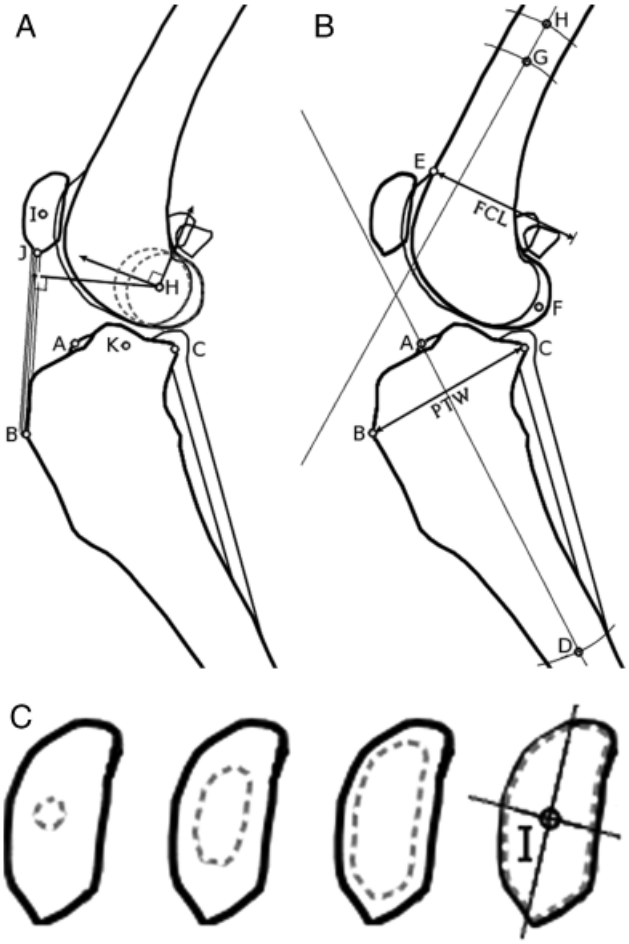

Figure 3 (A) Mediolateral view of the stifle joint illustrating the measurement of a femoral coordinate system: reference point on the tibia (K), reference point on the patella (I), and the patellar tendon moment arm (HJ). The origin of the coordinate system (H) was positioned at the estimated center of rotation of the stifle (placed midway between the centers of 2 circles fit to the posterior femoral condyles). A proximal reference axis was constructed parallel to the anatomical axis of the distal femur and a cranial reference axis was constructed orthogonal to the plane of the image and the proximal axis. Patellar tendon moment arm (perpendicular distance from the femoral origin to the line of action of the patellar tendon), position of the tibia (midpoint between the most cranial (A) and caudal (C) points of the tibial articulating surface) and the patella position (estimated centroid of the patella) were measured with respect to the femoral coordinate system. (B) Illustration of topology adaptive snake algorithm used to determine the patellar centroid and axes. Numerical optimization was used to 'inflate' the snake to best fit the radiographic outline of the patella, resulting in a uniformly sampled contour surrounding the patella. The centroid of this contour (I) and the principle contour axes were computed. (C) Mediolateral view of the stifle joint illustrating the measurement of anatomical axes for the proximal tibia and distal femur utilizing the proximal tibial width (PTW) and the femoral condyle length (FCL) to construct arcs which intersect the distal tibial cortex and proximal femoral cortex, respectively.

was defined as the line connecting the cranial aspect of the articular surface and the midpoint between the intersections of the arc and each cortex. The stifle joint angle was defined as the angle between the long axes of the distal femur and proximal tibia (Fig 3C).

A coordinate measurement system was defined on the distal femur (Fig 3A). Both medial and lateral femoral condyles were approximated using best-fit circles. A right-handed Cartesian coordinate system was fixed to the femur having an origin located at the midpoint of the medial and lateral best-fit circle centers.[45] The proximal axis was constructed parallel to the long axis of the distal femur directed proximally positive. The cranial axis was taken orthogonal to the proximal axis and the plane of the radiograph directed cranially positive. The position of the tibia was defined by the midpoint of the most cranial aspect of the articular surface of the proximal tibia and the most caudal aspect of the tibial condyles, measured with respect to the femoral coordinate system.

A topology adaptive snake algorithm, based on a deformable active contour model,[46] was implemented to determine the approximate silhouette of the patella (Fig 3B). A set of seed points within the boundaries of the patella was used to initialize the contour. Numerical optimization was used to 'inflate' the snake to best fit the radiographic outline of the patella, resulting in a uniformly sampled contour surrounding the patella. The position of the patella, measured in mm, was defined as the centroid of this contour and the principle contour moments were computed to determine major/minor elliptical axes of the patella (Fig 3B). Patellar tilt, measured in degrees, was defined as the angle between the long axes of the distal femur and patella. The patellar tendon moment arm, measured in mm, was defined as the perpendicular distance from the femoral origin to the line of action of the patellar tendon.

Statistical Analysis

Data editing and statistical analyses were performed using Stata Software (StataCorp., 2009; Stata Statistical Software: Release 10.1; College Station, TX). Differences in cranial translation of the tibia, patellar displacement, contact area, peak pressure, mean pressure, and total force between conditions were compared in the following way: Peak pressure location, patellar displacement, and cranial translation of the tibia were measured and expressed in mm from the intact condition which was defined as 0. Contact area, peak and mean pressure magnitude, and total force were normalized to the measurements obtained in the intact condition, which were defined as 100%. After normalization these values were expressed as a percentage of the intact condition.

Analysis 1: A 1-sample 2-sided t-test was performed when using a baseline-normalized comparison. Therefore the baseline was set for each individual to100 or 0. Thus, the intact condition (i.e., baseline) was compared with CrCLT and to TTA conditions. Bonferroni's correction ($\beta = \alpha/\eta = 0.0167$) was performed.

Analysis 2: A paired t-test was performed between CrCLT and TTA conditions. If using percentages, a Wilk–Shapiro test was used to check for normality distribution before performing a parametric analysis.

Analysis 3: Changes in stifle extension angles between conditions were assessed using general linear model, where angle was the dependent variable, and the condition (Intact, CrCLT, and TTA) was entered as independent variable. It was assumed that all variances were equal and covariance was zero. Since the variable distribution was tested for normality, the error was also assumed to be normally distributed.

Analysis 4: Two separate ANOVAs with repeated measures were conducted to assess differences in PF and FT poses data between treatment conditions (i.e., normal, CrCLT, and TTA). When appropriate, pairwise comparisons for treatment groups were corrected using a Bonferroni adjustment.

For all statistical analyses performed, $P \leq .05$ was considered statistically significant. When Bonferroni correction was used, $P \leq .0167$ was considered statistically significant.

RESULTS

The study was performed in 9 stifles of 6 dogs (mean body weight, 41.7 kg [range, 25–63 kg]). Based on preoperative planning, cages of 9 mm (6) and 12 mm (3 cases) were used.

Contact area, peak contact pressure and location, mean pressure and total force values (mean ± SD) are presented in Table 1. Contact area and peak contact pressure were not statistically different among the 3 conditions. Peak contact location was found to be significantly more proximal in the CrCLT condition than in the intact condition ($P = .002$; Fig 4) After Bonferroni correction no

Table 1 Patellofemoral Contact Mechanics for Normal, CrCLT, and TTA-Treated Conditions after Normalizing Values

Parameter	Normal (1)	CCLT (2)	TTA-Treated (3)
Contact area (%)	(100)	98.74 ± 11.31 ($P_{1-2} = 0.74$)	95.3 ± 16.84 ($P_{1-3} = 0.42$, $P_{2-3} = 0.49$)
Peak pressure magnitude (%)	(100)	84.17 ± 31.56 ($P_{1-2} = 0.17$)	93.13 ± 23.73 ($P_{1-3} = 0.41$, $P_{2-3} = 0.36$)
Peak pressure location (mm)	(0)	4.40 ± 3.12 (**$P_{1-2} = 0.002$**)	1.77 ± 2.9 ($P_{1-3} = 0.1$, $P_{2-3} = 0.02$)
Mean pressure (%)	(100)	73.34 ± 12.44 (**$P_{1-2} \leq 0.001$**)	85.09 ± 15.18 ($P_{1-3} = 0.018$, $P_{2-3} = 0.065$)
Total force (%)	(100)	71.20 ± 10.66 (**$P_{1-2} \leq 0.001$**)	78.88 ± 9.51 (**$P_{1-3} \leq 0.001$**, $P_{2-3} = 0.065$)

Values are expressed in percentage of the normal condition. The results of peak pressure displacement are expressed in mm.
P-values are bolded where significant differences were detected after Bonferroni correction ($\beta = \alpha/\eta = 0.0167$).
CrCLT, cranial cruciate ligament transection; TTA, tibial tuberosity advancement.

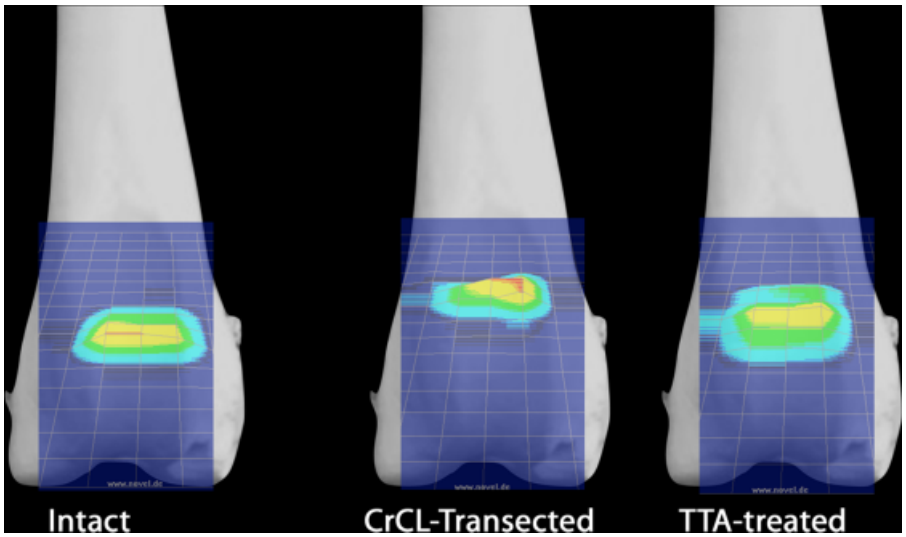

Figure 4 An example of contact maps obtained from the Novel software representative of each testing condition, depicted over an axial view of the femoral sulcus. The software is able to define peak pressure location in one sensel and to provide the map in a grid that allows for measurement of displacements.

statistically significant difference in peak contact location could be found comparing intact and TTA-treated conditions ($P = .1$) and between CrCLT- and TTA-treated conditions ($P = .02$). The mean pressure acting in the retropatellar area decreased significantly from intact to CrCLT ($73.34 \pm 12.44\%$; $P \leq .001$).). After Bonferroni correction, the decrease in retropatellar pressure from intact to TTA-treated stifles ($85.09 \pm 15.18\%$; $P = .018$) was not statistically significant. The difference in retropatellar pressure between CrCLT- and TTA-treated conditions was also not statistically significant ($P = .065$). The total force acting in the PF joint decreased significantly from intact to CrCLT- ($71.20 \pm 10.66\%$; $P \leq .001$) and TTA-treated ($78.88 \pm 9.51\%$; $P \leq .001$) conditions. No statistically significantly differences were found between CrCLT- and TTA-treated conditions ($P = .065$).

Mediolateral radiographs showed no variation in the position of the pressure sensors during testing. Based on the radiopaque bone markers no proximo-distal displacement of the patella relative to the femur could be detected. As determined by the general linear model stifle angles did not vary between the intact ($123.27 \pm 4.34^{\circ}$), CrCLT- ($122.08 \pm 5.10^{\circ}$), and TTA-treated ($124.23 \pm 6.48^{\circ}$) conditions. Measurement of the tibial translation using the radiopaque markers demonstrated a cranial tibial displacement of 9.35 ± 1.19 mm after CrCLT. The subluxation was corrected in the TTA-treated condition with measured values of -0.46 ± 2.09 mm. The differences in FT distance between intact and CrCLT conditions ($P < .001$), and between CrCLT- and TTA-treated were statistically significant ($P < .001$). No significant difference was detected between intact and TTA-treated conditions ($P = .52$).

The values describing the FT and PF poses (mean $\pm$ SD) calculated with the digitization method are presented in Table 2. CrCLT caused a significant craniocaudal and proximodistal translation of the tibia and altered the patellar tilt angle ($P < .01$). TTA re-established FT and PF alignments, which were not different from the control. The moment arm of the patellar tendon significantly increased from the control in both CrCLT- and TTA-conditions ($P < .01$).

DISCUSSION

We found that CrCL-deficient stifles have altered PF alignment and contact mechanics. These changes in PF

Table 2 Static 2-Dimensional Femorotibial and Patellofemoral Poses for Normal, CrCL-Deficient, and TTA-Treated Conditions

Parameter	Normal (1)	CCLT (2)	TTA-Treated (3)
Tibial craniocaudal translation (mm)	-9.3 ± 1.5	-1.63 ± 1.2 ($\mathbf{P_{1-2} \leq 0.001}$)	-9.4 ± 1.7 ($\mathbf{P_{2-3} \leq 0.001}$)
Tibial superinferior translation (mm)	-12.4 ± 2.0	-17.7 ± 2.4 ($\mathbf{P_{1-2} \leq 0.001}$)	-12.5 ± 2.3 ($\mathbf{P_{2-3} \leq 0.001}$)
Patellar craniocaudal translation (mm)	40.5 ± 6.3	40.9 ± 6.6	40.6 ± 6.5
Patellar superoinferior translation (mm)	0.9 ± 2.8	0.9 ± 3.1	0.3 ± 3.9
Patellar tilt angle (°)	31.3 ± 4.4	35.4 ± 4.6 ($\mathbf{P_{1-2} \leq 0.001}$)	32.9 ± 4.6
Moment arm (mm)	32.1 ± 4.6	35.5 ± 5.3 ($\mathbf{P_{1-2} \leq 0.001}$)	35.7 ± 5.1 ($\mathbf{P_{1-3} \leq 0.001}$)

For the translational variables, positive values indicate cranial and distracted positions of the tibia relative to the femur. *P*-values for *post hoc* pairwise comparisons are given where significant differences were detected by the ANOVAs. *P*-values are bolded where significant differences were detected. CrCLT, cranial cruciate ligament transection; TTA, tibial tuberosity advancement.

biomechanics may predispose to PF osteoarthritis after CrCL rupture. In addition we found that TTA restored the normal FT and PF alignment, and reduced the retropatellar forces by about 20% and the retropatellar pressure by 15%. We suspect that the decrease in retropatellar force may be due to the increased moment arm of the patellar tendon after TTA, rather than a cranial translation of the patella relative to the femur. The decreased retropatellar force after TTA may have beneficial effects in dogs with CrCL insufficiency, but this speculation needs to be confirmed with in vivo studies.

Osteoarthritis is a mechanically induced disorder in which the consequences of abnormal joint mechanics provoke biologic effects that are mediated biochemically, for example through cytokines, matrix-degrading enzymes and toxic oxygen radicals.[47] In our study we found that CrCL transection altered both alignment and contact mechanics of the PF joint. Our findings are consistent with previous in vivo experiments performed in cats. Hasler et al reported that after CrCL transection the resultant PF contact forces were decreased by approximately 30%.[48] This decrease was primarily caused by the decreased extensor force acting on the PF joint.[48] Our results showed a 20% decrease in retropatellar force after CrCLT, and a significantly increased moment arm of the patellar tendon compared with the intact stifle. The increase in moment arm is expected to produce a lower extensor force, resulting in reduced stifle loading as suggested in previous in vivo studies.[48,49] Similar findings were also reported by Shahar et al[50] in a mathematical model of the canine stifle. Based on our results and previous studies,[48–50] it could be speculated that unloading and altering contact points and alignment of the joint, rather than overloading might predispose to PF osteoarthritis in dogs.

In both CrCLT- and TTA-treated stifles retropatellar force and pressure decreased to about 75% of the value measured in the control stifle. However, the 2 conditions differed significantly because in the CrCLT stifles an abnormal tilt angle and a proximal shift of PF peak pressure were noted, whereas no other abnormalities in contact mechanics and poses were observed after TTA. While alteration of both contact mechanics and joint poses can be considered a risk factor for osteoarthritis in the CrCLT stifle,[51] the decrease in retropatellar force after TTA may be advantageous in a joint with existing osteoarthritis for decreasing pain and slowing progression of cartilage degeneration.[21,26,30] In people with unicompartmental osteoarthritis, tibial osteotomy decreases joint loads and slows the progression of cartilage breakdown in the affected compartment.[52] Similarly, TTA may be beneficial in dogs with PF osteoarthritis for its effect on retropatellar force. Our speculations are supported by the theory proposed by Andriacchi et al[51] on pathomechanics of osteoarthritis. In the initiation phase, kinematic abnormalities cause a shift in load bearing regions. Consequently contact pressures decrease in regions normally loaded, and increase in infrequently loaded regions. The progression phase is characterized by more rapid progression with increased loads. In our study the pressure shift and abnormal PF pose in the CrCL-deficient stifle would act as trigger for osteoarthritis. In the progression phase, TTA may be beneficial because it lowers the retropatellar forces. However, these results need to be confirmed in vivo.

The moment arm of the knee-extensor mechanism is described by the moment arm of the patellar tendon calculated with respect to the screw axis of the tibia relative to the femur.[53] The moment arm may be found once the line of action of the patellar tendon and the position and orientation of the screw axis are known. Previous studies have obtained moment arms of the patellar tendon referenced to the contact point between the femur and tibia.[54,55] The contact point may not be meaningful because this point itself is rotating about the screw axis.[53] In this study, we followed a similar method to Smidt[56] who measured the moment arm with respect to the axis of rotation of the FT joint. We calculated the center of rotation of the stifle using an average of the center of 2 circles estimating the curvature of the femoral condyles. This is an approximation of the true center of rotation because our analysis assumed that the bones moved only in the sagittal plane and, therefore, did not take into account axial rotation of the tibia relative to the femur during knee extension. Furthermore, the true center of rotation would move as the joint flexes. A more correct method would be to calculate the moment arm of the PF joint in 3 dimensions, to eliminate the effect of out-of-plane rotations of the bone.[53] In this study the moment arm increased significantly in both CrCLT- and TTA-treated stifles. This finding is consistent with the decrease in retropatellar forces measured in both conditions, as an increase in moment arm corresponds to a decrease in quadriceps force.

The PF and FT poses were measured using a custom computer digitization technique designed to construct a femoral coordinate system to measure the positions of the patella and tibia relative to the femur. In general, digitization techniques that allow for high magnification during data collection have improved repeatability and precision. One specific advantage of this method is that a coordinate system based on the center of rotation of the joint should be minimally influenced by changes in joint angles. In this study we calculated the femoral coordinate system with a similar method to the Joint Coordinate System described by Grood and Suntay.[57] The center of the coordinate system in this study is an estimation of the center of rotation of the joint, but cannot be considered a true instantaneous center of rotation because it was calculated at a single flexion joint angle. The centers of the medial and lateral femoral coordinates were selected because they were found to be the best anatomical landmarks using the digitization software. In addition, this method allowed for measurements of the PF poses utilizing the entire geometry of the patella. Previous methods used a subset of points along the boundary of the patella in order to express the patellar axis and centroid.[58]

During the experimentation, stifle angle was measured as described previously,[40] using as landmarks the greater

trochanter of the femur, the FT joint between the lateral epicondyle of the femur and the fibular head, and the lateral malleolus of the distal tibia.[40] Being the radiographs centered in the stifle and not large enough to repeat the same measurements, we had to measure stifle extension from landmarks taken from the distal femur and proximal tibia, as described in previous studies.[43,44] The different landmarks used between experiment and measurement from radiographs explains why the angles reported here are smaller than the angles used in the experimental phase. Only a single angle of stifle extension was used in this study. It represents the mean angle of extension of the FT joint during the stance phase of the gait.[40] Having the stifle a range of motion of approximately 23° during this phase,[40] we assume that retropatellar forces would be reduced during all the stance phase of the gait. We cannot extrapolate our results to other situations in which the stifle undergoes more flexion (i.e. sitting, standing up), or other activities such as jumping or turning.

Caution must be taken when extrapolating the results of an in vitro study to in vivo conditions. Joint flexion and extension results from muscular co-contraction, and the combined action of the muscles about the stifle can increase the joint reaction forces to higher values than what we measured. The kerf of the blade was not accounted during our study. A narrow saw blade was used to perform the osteotomies, and being the advancement planed before the osteotomy took place, the thickness of bone removed was the same in the 3 situations and therefore shouldn't alter results expressed in percentage. In the present study, a pressure sensor was positioned in the retropatellar area, slightly modifying its position, and stifles were loaded at a single position of extension and under a single load selected to simulate the joint forces presumed to occur in vivo under certain conditions of activity. This represents only a fraction of the normal range of motion and loading forces. By measuring 2-dimensional poses of the PF and FT joints, we assume that these joints move only on the sagittal plane. While the PF joint may have minimal internal external rotation, the more complex FT joint has 6 degrees of freedom.[49] A 3-dimensional methodology would have considered all of the relevant rotations and translation of the stifle. Furthermore, 3-dimensional analysis of PF poses would allow a more precise evaluation of the extensor mechanism moment arm. The model used here is a gross simplification of what occurs in nature, and therefore our results have to be interpreted carefully and should be confirmed with in vivo studies.

Ex vivo studies on joint contact mechanics are controversial because they cannot simulate the complex history of the cartilage loading during everyday life activity. In addition, static studies ignore contact shear stress that may be more significant than the simple compression stress acting on the cartilage. However, in vivo contact pressures cannot be measured in animals or people. Thus, cadaveric studies may provide useful information by measuring the changes in joint surface pressures in a controlled experimental set-up. Based on our results we suggested that abnormal mechanical loading and joint alignment might predispose to PF osteoarthritis in dogs. We also speculate that TTA may be beneficial in dogs with PF osteoarthritis for its effect on retropatellar force, with a similar mechanism to pressure-shifting high tibial osteotomies.[52] Further studies are needed to confirm if these results obtained in a cadaveric model also apply to clinical cases. In addition, further studies are needed to evaluate effect of over/under contouring of the TTA plate in lateral and medial PF contact mechanics.

ACKNOWLEDGMENTS

Study supported by a grant from the University of Zurich.

REFERENCES

1. Conzemius MG, Evans RB, Besancon MF, et al: Effect of surgical technique on limb function after surgery for rupture of the cranial cruciate ligament in dogs. *J Am Vet Med Assoc* 2005;226:232–236
2. Corr SA, Brown C: A comparison of outcomes following tibial plateau levelling osteotomy and cranial tibial wedge osteotomy procedures. *Vet Comp Orthop Traumatol* 2007;20:312–319
3. Guenego L, Zahra A, Madelenat A, et al: Cranial cruciate ligament rupture in large and giant dogs. A retrospective evaluation of a modified lateral extracapsular stabilization. *Vet Comp Orthop Traumatol* 2007;20:43–50
4. Chauvet AE, Johnson AL, Pijanowski GJ, et al: Evaluation of fibular head transposition, lateral fabellar suture, and conservative treatment of cranial cruciate ligament rupture in large dogs: a retrospective study. *J Am Anim Hosp Assoc* 1996;32:247–255
5. Boudrieau RJ: Tibial plateau leveling osteotomy or tibial tuberosity advancement? *Vet Surg* 2009;38:1–22
6. Tepic S, Damur DM, Montavon PM: Biomechanics of the stifle joint, *Proceedings of the 1stWorld Orthopedic Veterinary Congress ESVOT-VOS*, Munich, Germany, pp 189–190, 2002
7. Montavon PM, Damur DM, Tepic S: Advancement of the tibial tuberosity for the treatment of cranial cruciate deficit canine stifle, *Proceedings of the 1st World Orthopedic Veterinary Congress ESVOT-VOS*, Munich, Germany, p 152, 2002
8. Guerrero TG: Advancement of the tibial tuberosity for the treatment of cranial cruciate-deficient canine stifle. Materials, principles and surgical procedure. Doctoral Thesis. University of Zurich, 2003
9. Kim SE, Pozzi A, Banks SA, et al: Effect of tibial tuberosity advancement on femorotibial contact mechanics and stifle kinematics. *Vet Surg* 2009;38:33–39
10. Miller JM, Shires PK, Lanz OI, et al: Effect of 9 mm tibial tuberosity advancement on cranial tibial translation in the canine cranial cruciate ligament-deficient stifle. *Vet Surg* 2007;36:335–340
11. Kipfer NM, Tepic S, Damur DM, et al: Effect of tibial tuberosity advancement on femorotibial shear in cranial cruciate-deficient stifles. An in vitro study. *Vet Comp Orthop Traumatol* 2008;21:385–390

12. Apelt D, Kowaleski MP, Boudrieau RJ: Effect of tibial tuberosity advancement on cranial tibial subluxation in canine cranial cruciate-deficient stifle joints: an in vitro experimental study. *Vet Surg* 2007;36:170–177
13. Dennler R, Kipfer NM, Tepic S, et al: Inclination of the patellar ligament in relation to flexion angle in stifle joints of dogs without degenerative joint disease. *Am J Vet Res* 2006;67:1849–1854
14. Voss K, Damur DM, Guerrero T, et al: Force plate gait analysis to assess limb function after tibial tuberosity advancement in dogs with cranial cruciate ligament disease. *Vet Comp Orthop Traumatol* 2008;21:243–249
15. Adams ME: Cartilage hypertrophy following canine anterior cruciate ligament transection differs among different areas of the joint. *J Rheumatol* 1989;16:818–824
16. Chester R, Smith TO, Sweeting D, et al: The relative timing of VMO and VL in the aetiology of anterior knee pain: a systematic review and meta-analysis. *BMC Musculoskelet Disord* 2008;9:64, doi: 10.1186/1471-2474-9-64
17. Houghton KM: Review for the generalist: evaluation of anterior knee pain. *Pediatr Rheumatol Online J* 2007;5:8, doi: 10.1186/1546-0096-5-8
18. Hull JB, Hobbs C, Sidebottom S: Anterior knee pain syndrome. A review of current concepts and controversies. *J R Army Med Corps* 1999;145:89–94
19. Lattermann C, Drake GN, Spellman J, et al: Lateral retinacular release for anterior knee pain: a systematic review of the literature. *J Knee Surg* 2006;19:278–284
20. Witonski D: Anterior knee pain syndrome: a historical review. *Chir Narzadow Ruchu Ortop Pol* 1998;63:379–385
21. Maquet P: Advancement of the tibial tuberosity. *Clin Orthop Relat Res* 1976;115:225–230
22. Ferguson AB Jr., Brown TD, Fu FH, et al: Relief of patellofemoral contact stress by anterior displacement of the tibial tubercle. *J Bone Joint Surg Am* 1979;61:159–166
23. Huber JGB, Perren SM, Bandi W: Changes in retropatellar pressure values in relation to the position of the tibial tuberosity. *Knee* 1994;1(Suppl. II): 19–43
24. Singerman R, White C, Davy DT: Reduction of patellofemoral contact forces following anterior displacement of the tibial tubercle. *J Orthop Res* 1995;13:279–285
25. Shirazi-Adl A, Mesfar W: Effect of tibial tubercle elevation on biomechanics of the entire knee joint under muscle loads. *Clin Biomech* 2007;22:344–351
26. Rue JPH, Colton A, Zare SM, et al: Trochlear contact pressures after straight anteriorization of the tibial tuberosity. *Am J Sports Med* 2008;36:1953–1959
27. Ferrandez L, Usabiaga J, Yubero J, et al: An experimental study of the redistribution of patellofemoral pressures by the anterior displacement of the anterior tuberosity of the tibia. *Clin Orthop Relat Res* 1989;238:183–189
28. Hirsh DM, Reddy DK: Experience with Maquet anterior tibial tubercle advancement for patellofemoral arthralgia. *Clin Orthop Relat Res* 1980;148:136–139
29. Mendes DG, Soudry M, Iusim M: Clinical assessment of Maquet tibial tuberosity advancement. *Clin Orthop Relat Res* 1987;222:228–238
30. Schmid F: The Maquet procedure in the treatment of patellofemoral osteoarthrosis. Long-term results. *Clin Orthop Relat Res* 1993;294:254–258
31. Ferguson AB Jr: Elevation of the insertion of the patellar ligament for patellofemoral pain. *J Bone Jt Surg Am* 1982;64:766–771
32. Schmoekel H, Montavon PM: Versetzung der Tuberositas tibiae mit einer Kranialisation bei der Patellaluxation beim Hund. *Kleintierpraxis* 1993;38:805–808
33. Koch DA, Montavon PM: Clinical experiences with the therapy for patella luxation of small animals using sulcoplasty and lateral and cranial relocation of the tuberositas tibiae. *Schweiz Arch Tierheilkd* 1997;139:259–264
34. ĹEplattenier H, Montavon PM: Patellar luxation in dogs and cats: management and prevention. *Compend Contin Educ Pract Vet* 2002;24:292–298
35. Tepic S, Montavon PM: Is cranial tibial advancement relevant in the cruciate deficient stifle? *Proceedings of the 12th ESVOT Congress*, Munich, Germany, pp 132–133, 2004
36. Kim SE, Pozzi A, Kowaleski MP, et al: Tibial osteotomies for cranial cruciate ligament insufficiency in dogs. *Vet Surg* 2008;37:111–125
37. Hoffmann DE, Miller JM, Ober CP, et al: Tibial tuberosity advancement in 65 canine stifles. *Vet Comp Orthop Traumatol* 2006;19:219–227
38. Lafaver S, Miller NA, Stubbs WP, et al: Tibial tuberosity advancement for stabilization of the canine cranial cruciate ligament-deficient stifle joint: surgical technique, early results, and complications in 101 dogs. *Vet Surg* 2007;36:573–586
39. Hoffmann DE, Kowaleski MP, Johnson KA, et al: In vitro biomechanical evaluation of the canine CrCL deficient stifle with varying angles of stifle joint flexion and axial loads after TTA. *Proceedings of the 36thAnnual Conference Veterinary Orthopedic Society*, Steamboats springs, CO, p 1, 2009
40. Hottinger HA, DeCamp CE, Olivier NB, et al: Noninvasive kinematic analysis of the walk in healthy large-breed dogs. *Am J Vet Res* 1996;57:381–388
41. DeCamp CE, Riggs CM, Olivier NB, et al: Kinematic evaluation of gait in dogs with cranial cruciate ligament rupture. *Am J Vet Res* 1996;57:120–126
42. Roos PJ, Neu CP, Hull ML, et al: A new tibial coordinate system improves the precision of anterior-posterior knee laxity measurements: a cadaveric study using Roentgen stereophotogrammetric analysis. *J Orthop Res* 2005;23:327–333
43. Mostafa AA, Griffon DJ, Thomas MW, et al: Morphometric characteristics of the pelvic limbs of Labrador Retrievers with and without cranial cruciate ligament deficiency. *Am J Vet Res* 2009;70:498–507
44. Abel SB, Hammer DL, Shott S: Use of the proximal portion of the tibia for measurement of the tibial plateau angle in dogs. *Am J Vet Res* 2003;64:1117–1123
45. Kurosawa H, Walker PS, Abe S, et al: Geometry and motion of the knee for implant and orthotic design. *J Biomech* 1985;18:487–499
46. Kass M WA, Terzopoulos D: Snakes: active contour models. *Int J Comput Vision* 1988;1:321–331

47. Griffin TM, Guilak F: The role of mechanical loading in the onset and progression of osteoarthritis. *Exerc Sport Sci Rev* 2005;33:195–200

48. Hasler EM, Herzog W: Quantification of in vivo patellofemoral contact forces before and after ACL transection. *J Biomech* 1998;31:37–44

49. Korvick DL, Pijanowski GJ, Schaeffer DJ: Three-dimensional kinematics of the intact and cranial cruciate ligament-deficient stifle of dogs. *J Biomech* 1994;27:77–87

50. Shahar R, Banks-Sills L: A quasi-static three-dimensional, mathematical, three-body segment model of the canine knee. *J Biomech* 2004;37:1849–1859

51. Andriacchi TP, Mundermann A, Smith RL, et al: A framework for the in vivo pathomechanics of osteoarthritis at the knee. *Ann Biomed Eng* 2004;32:447–457

52. Majima T, Yasuda K, Katsuragi R, et al: Progression of joint arthrosis 10 to 15 years after high tibial osteotomy. *Clin Orthop Relat Res* 2000;381:177–184

53. Krevolin JL, Pandy MG, Pearce JC: Moment arm of the patellar tendon in the human knee. *J Biomech* 2004;37: 785–788

54. Herzog W, Read LJ: Lines of action and moment arms of the major force-carrying structures crossing the human knee joint. *J Anat* 1993;182(Part 2): 213–230

55. Nisell R: Mechanics of the knee. A study of joint and muscle load with clinical applications. *Acta Orthop Scand* 1985; 216(Suppl.): 1–42

56. Smidt GL: Biomechanical analysis of knee flexion and extension. *J Biomech* 1973;6:79–92

57. Grood ES, Suntay WJ: A joint coordinate system for the clinical description of three-dimensional motions: application to the knee. *J Biomech Eng* 1983;105:136–144

58. Stiehl JB, Komistek RD, Dennis DA, et al: Kinematics of the patellofemoral joint in total knee arthroplasty. *J Arthroplasty* 2001;16:706–714